Intracellular O_2 Sensing Probe Based on Cell-Penetrating Phosphorescent Nanoparticles

Andreas Fercher,[†] Sergey M. Borisov,[‡] Alexander V. Zhdanov,[†] Ingo Klimant,[‡] and Dmitri B. Papkovsky[†,*]

[†]Biochemistry Department, University College Cork, Cavanagh Building, College Road, Cork, Ireland, and [‡]Institute of Analytical Chemistry & Food Chemistry, Graz University of Technology, 8010 Graz, Austria

ABSTRACT A new intracellular O_2 (icO_2) sensing probe is presented, which comprises a nanoparticle (NP) formulation of a cationic polymer Eudragit RL-100 and a hydrophobic phosphorescent dye Pt(II)-tetrakis(pentafluorophenyl)porphyrin (PtPFPP). Using the time-resolved fluorescence (TR-F) plate reader set-up, cell loading was investigated in detail, particularly the effects of probe concentration, loading time, serum content in the medium, cell type, density, *etc.* The use of a fluorescent analogue of the probe in conjunction with confocal microscopy and flow cytometry analysis, revealed that cellular uptake of the NPs is driven by nonspecific energy-dependent endocytosis and that the probe localizes inside the cell close to the nucleus. Probe calibration in biological environment was performed, which allowed conversion of measured phosphorescence lifetime signals into icO_2 concentration (μM). Its analytical performance in icO_2 sensing experiments was demonstrated by monitoring metabolic responses of mouse embryonic fibroblast cells under ambient and hypoxic macroenvironment. The NP probe was seen to generate stable and reproducible signals in different types of mammalian cells and robust responses to their metabolic stimulation, thus allowing accurate quantitative analysis. High brightness and photostability allow its use in screening experiments with cell populations on a commercial TR-F reader, and for single cell analysis on a fluorescent microscope.

KEYWORDS: nanoparticle sensors · intracellular oxygen · cell-penetrating probe · cell respiration · metabolism · time-resolved fluorescence · fluorescent oxygen imaging · phosphorescence quenching

In recent years there has been a major progress in our understanding of cellular function and the processes taking place in normal and diseased cells and tissues. To a large degree this was due to the development of new detection technologies (spectroscopy, `omics', live cell and intravital imaging), accessory biomaterials (chemistries, probes, biosensors) and analytical procedures. As a result, a significant number of cellular parameters are now amenable to routine analysis, including real-time live cell monitoring.[1] However, some "difficult" analytes still remain, and this list includes molecular oxygen (O_2). O_2 is the key substrate and source of energy for the cell which is involved in many pathophysiological conditions and adaptive responses to hypoxia.[2,3] This small gaseous analyte diffuses quickly in solution, in and out of the cell, and is present in vast excess in the environment. Although O_2 can be "sensed" with good selectivity and sensitivity by a number of techniques,[4,5] including phosphorescence quenching,[6,7] its accurate detection particularly in biological samples, on a microscale, and within the cell represents a significant challenge.[8,9]

Measurement of O_2 and its consumption by means of phosphorescent solid-state (micro)sensors[10] or extracellular probes[11,12] is relatively well established. However, monitoring of intracellular O_2 (icO_2) is gaining increasing interest particularly with the view of mechanistic studies of cell respiration, metabolism, gene expression, various diseases, and drug effects.[13] The monitoring of icO_2 can provide real-time information on cell oxygenation, its mitochondrial function, and bioenergetic status. Therefore, development of simple and efficient probe chemistries, cell loading, and measurement procedures is important.

Thus far, icO_2 sensing has been demonstrated with a number of supramolecular[14−16] and particle-based probes,[17−19] which were introduced into the cells by gene gun[18] microinjection[14,17,20] facilitated macropinocytosis or induced endocytosis[16] and then measured by different means. However, complex probe chemistries, inefficient and cumbersome cell loading procedures (rather low, time-consuming, invasive, and stressful for the cells) and/or inadequate analytical performance, limited severely the use of such probes. More recently, O_2 probes with self-loading capabilities have been described, particularly those based on Pt(II)—coproporphyrin dye conjugated to cell-penetrating peptides (oligo-arginine and bactenecin),[21,22] which showed high self-loading efficiency and good performance in icO_2 sensing in conjunction with time-resolved

* Address correspondence to d.papkovsky@ucc.ie.

Received for review February 28, 2011 and accepted June 14, 2011.

Published online June 14, 2011
10.1021/nn200807g

fluorometry. Other approaches include ratiometric luminescent nanoparticles coated with cell-penetrating peptides or amino groups.[23,24] Despite the improvements achieved with these probes, they still possess drawbacks such as significant degree of cell-specificity; insufficient photostability and brightness which make them problematic for O_2 imaging applications where high illumination intensities and long time-lapse experiments are commonly used; rather complex synthesis; and significant costs.

We present a new icO_2 probe which overcomes many limitations of existing probes. The probe, which comprises a nanoparticle (NP) formulation of a cationic polymer Eudragit RL-100[25] and a phosphorescent dye Pt(II)-*meso*-tetrakis-(pentafluorophenyl)porphyrin (PtPFPP),[26] shows excellent self-loading capabilities with various mammalian cells, very high brightness and photostability,[27] and low degree of cell specificity, along with general simplicity and convenience of use. The efficiency of cell loading, uptake mechanisms, and localization of PtPFPP NPs in different cells were investigated in detail. Subsequently, probe performance was demonstrated in icO_2 sensing experiments on standard spectroscopic equipment—time-resolved fluorescence (TR-F) reader and live cell fluorescence microscopy imaging, using mouse embryonic fibroblast cells (MEFs).

RESULTS AND DISCUSSION

Design and Spectral Characterization of the NP Probe. Eudragit RL-100 polymer was originally developed for use in biocompatible coatings and drug delivery systems.[25,28] Recently, it was used to produce optochemical sensor nanoformulations with photoluminescent indicators incorporated in RL-100 NPs by means of physical inclusion.[29] Such nanomaterials showed compatibility with different luminescent dyes, ease of preparation and use, reproducibility, and suitability for various (bio)analytical applications including general O_2 sensing. However thus far, such NP formulations have not been explored for sensing of icO_2 in live mammalian cells.

We hypothesized that significant net positive charge of the RL-100[30] and resulting NPs provide them the ability to interact with cell membrane (negatively charged outside) and penetrate inside the cells. In aqueous solutions, the PtPFPP NPs possess near-optimal sensitivity to O_2 covering the physiological range,[29] and spectral compatibility with standard TR-F readers and imaging systems (Figure 1a). These features make the PtPFPP-doped NPs a promising candidate for intracellular O_2 sensing applications. Moreover, high brightness (1.5% w/w dye content) and photostability provide them competitive advantages over the currently used cell-penetrating probes.[21,22]

To test this, we synthesized batches of PtPFPP-RL-100 NPs by the known method,[29] and examined them with

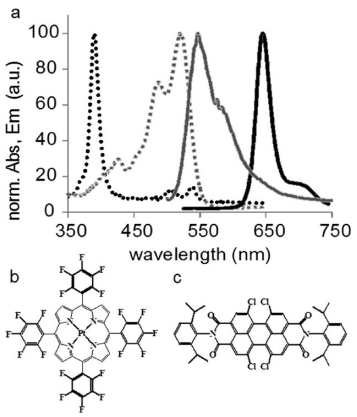

Figure 1. (a) Normalized absorption (dashed) and emission spectra (solid) of PtPFPP (black) and perylene (gray) NPs; chemical structures of (b) PtPFPP and (c) perylene dyes.

different mammalian cells, particularly with respect to their self-loading ability and analytical performance in icO_2 sensing experiments. Knowing that Pt−porphyrin-based probes are more difficult to use on confocal fluorescent imaging systems and flow cytometers (low luminescent signals since their long-decay emission is not very compatible with standard signal acquisition parameters), we also prepared RL-100 NPs impregnated with a fluorescent perylene dye. These were used to study NP loading and localization at a single-cell level.

Spectral characteristics of the two NP probes and dye structures are shown in Figure 1a−c. In a preliminary experiment, we measured phosphorescence lifetime of the PtPFPP NP probe (5 μg/mL) in air-saturated phosphate buffer having different pH values (range 6.0−8.0) and ionic strength (50 − 300 mM), at 37 °C. These parameters have no significant effect on probe lifetime, so its O_2 calibration remains stable in different media and environment (Supporting Information, Figure S1a). Temperature sensitivity is significant, as well-known from prior work,[6,7] and therefore should be accurately controlled. The absorption spectrum of the PtPFPP NP probe was identical to the monomeric PtPFPP,[26] proving that the dye does not aggregate.

NP morphology was analyzed by scanning electron microscope (SEM) and atomic force microscope (AFM) imaging which revealed that the particles have spherical shape, smooth surface, and an average particle size of 40 ± 12 nm and 35 ± 15 nm, respectively (Figure 2a,b), which was close to the particle size (~30 nm) obtained from the Zetasizer analyzer. This size of the NPs is smaller than for the majority of other O_2 nanoprobes (usually >100 nm).

Analysis of Self-Loading of the NP Probes. First, we studied the effects of probe concentration, loading time, cell density, and protein content in the medium on the loading of MEFs with PtPFPP NPs. In the previous studies with Pt−porphyrin-based O_2 probes, it has been worked out that TR-F intensity signals exceeding 3×10^4 cps

(counts per second) are required for reliable and accurate lifetime measurements in O_2 sensing experiments on a Victor reader with optimized settings.[16] Adherent MEFs grown as a monolayer on 96-well plate were incubated in Dulbecco's modified eagle medium (DMEM) with 1.25−40 μg/mL PtPFPP NPs for 12 h at 37 °C, then washed and measured. Figure 3a shows that high signals were achieved already with 1.25 μg/mL of the NPs (16 nM of PtPFPP). At higher concentrations (2.5−20 μg/mL) loading efficiency increased steadily without saturation, reaching the signals in excess of 400 000 cps (close to photodetector saturation). Kinetics of loading with 10 μg/mL PtPFPP NPs shows that the required TR-F signals can be generated already after 3 h incubation (Figure 3b) and that most of the signal increase occurs during the first 12 h of loading. These results were confirmed using perylene NPs and fluorescence activated cell sorter analysis (FACS), which produced a very similar pattern (Figure 3b).

To optimize cell concentration, we seeded MEFs at 1×10^4 to 4×10^4 cells/well, cultured them for 24 h, loaded with 10 μg/mL PtPFPP NPs for 12 h in DMEM at 37 °C, and then measured. Figure 3c shows that 3×10^4 cells/well can be regarded as optimal seeding concentration for O_2 sensing experiments.

Serum/protein content in the medium is known to affect transport of many probes and drug formulations into the cell.[31] We tested loading of MEFs with 10 μg/mL PtPFPP NPs at 50%, 10%, 3%, 1%, and 0% of fetal bovine serum (FBS). Although in the media with low serum content cell numbers were reduced (slower growth), the presence of the NP probe had no measurable effect on cell growth and total ATP levels (data not shown). At 50% FBS medium loading was inhibited by ~50% compared to 10% FBS (Figure 3d) which could be due to binding of albumin to the NPs preventing their interaction with cells. At the same time, probe signals remained sufficiently high for O_2 sensing experiments.

To investigate probe leakage from the cells, MEFs preloaded with PtPFPP NPs were cultured under standard culturing conditions for 24 h and measured periodically changing the medium prior to each measurement. Under these conditions, TR-F intensity and lifetime signals remained stable ($1.86 \pm 0.08 \times 10^5$ cps after 0 h and $1.96 \pm 0.1 \times 10^5$ cps after 24 h). Phosphorescence lifetime values for the respiring and nonrespiring (inhibited with antimycin A (AntiA)) MEFs were 33.82 ± 0.24 μs and 30.20 ± 0.17 μs, respectively. These results show that

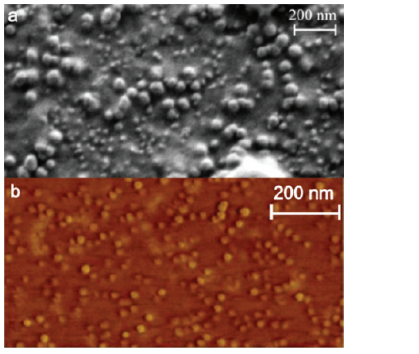

Figure 2. (a) SEM and (b) AFM images of the PtPFPP-RL100 NPs. Average particle size was determined to be 40 ± 12 nm and 35 ± 15 nm, respectively.

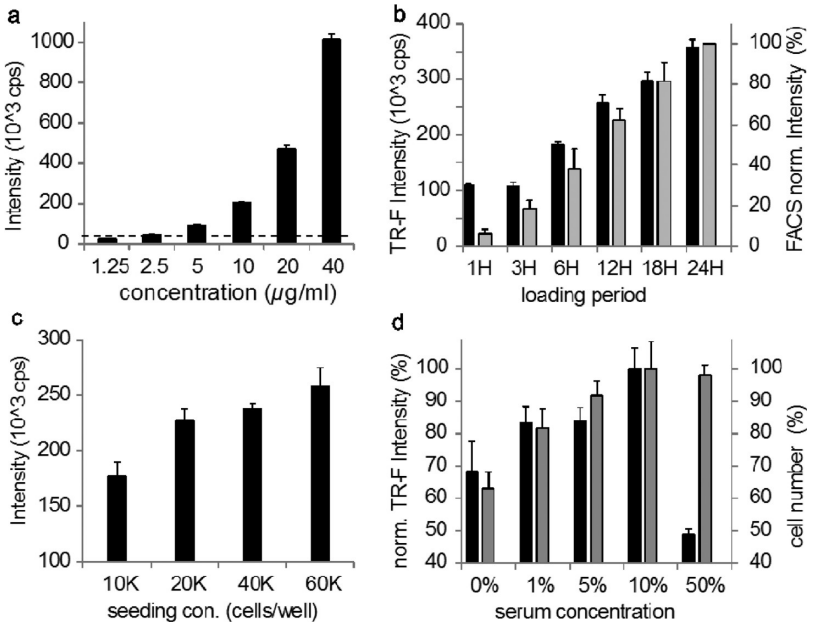

Figure 3. (a) TR-F intensity signals from MEFs loaded with 1.25−40 μg/mL PtPFPP NPs for 12 h (dashed line shows acceptable threshold signal). (b) Kinetics of MEFs loading with 10 μg/mL PtPFPP (black bars) and perylene (gray bars) doped NPs, presented as normalized mean TR-F and FACS GEO intensity signals, respectively. (c) TR-F intensity signals for MEFs seeded at different concentrations and loaded with 10 μg/mL PtPFPP NPs for 12 h. (d) The effect of serum content in the medium on the TR-F signals of MEFs loaded with PtPFPP NPs (black bars); relative cell numbers/ATP content are also shown (gray bars).

the NP probe does not leak from the cells and can be used over long periods of time. The absence of significant dye leaching was evident from the good storage stability of the probe (several months at 4 °C) and reproducible results of the O_2 sensing experiments. Also when precipitated by the addition of NaCl, the NPs retained the dye and the supernatant showed no characteristic absorbance of the PtPFPP. Dye leaching was tested under storage and physiological conditions: incubation of the NPs in PBS without and with 10% FBS, 37 °C followed by precipitation with salt. The dye was undetectable in the supernatant, so it does not leak.

Cytotoxic effects of PtPFPP NPs were assessed using luminescence-based ATP assay. In MEFs loaded with 5−20 μg/mL probe for ≤24 h or with ≤40 μg/mL for 14 h, ATP levels did not change significantly. Since unchanged ATP levels do not mean that cell bioenergetics remain unaffected,[12] we also conducted an extracellular acidification (ECA) assay, which showed no significant changes in glycolysis and (indirectly) in oxidative phosphorylation (OxPhos) after cell loading with the NP probe. Plasma membrane integrity assay showed no difference in the release of lactate dehydrogenase (LDH) enzyme from control and NPs loaded cells. This is consistent with the recent study of phototoxicity for the porphyrin-based nanoprobes, where the effects of sensitized singlet oxygen were seen negligible compared to the photodynamic drug Photofrin used at similar light doses.[11] Singlet oxygen can propagate ~100 nm in aqueous solution, so its damaging effect outside the polymeric NPs is expected to be minor. Small size and high brightness allow low probe concentrations to be used.

Altogether this shows that under standard experimental conditions PtPFPP NP probe had no detectable cytotoxicity or changes in cell viability (Supporting Information, Figure S1). At the same time, very high probe concentrations (≥40 μg/mL) did induce morphological changes in cells, detachment from the substrate and formation of clusters, therefore they should be avoided.

Finally, to show broader applicability of the NP probe based on RL-100 polymer, loading of several other cell lines, including human epithelial carcinoma (HeLa), human hepatocellular liver carcinoma (HepG2), nondifferentiated and differentiated human neuroblastoma (SH-SY5Y) and rat pheochromocytoma (PC12) cells was investigated. They all showed loading efficiency and localization patterns similar to MEF cells (Supporting Information, Figure S2). It is worth noting that in all these experiments emission lifetime of resting MEF cells seeded with 3×10^4 cells/per well and loaded after 24 h with PtPFPP NP probe for 12 h remained constant: 33.81 ± 0.25 μs. These data illustrate broad cell specificity of the NP probe. Based on this optimization, further experiments were performed with subconfluent cell monolayers grown in 10% FBS medium,

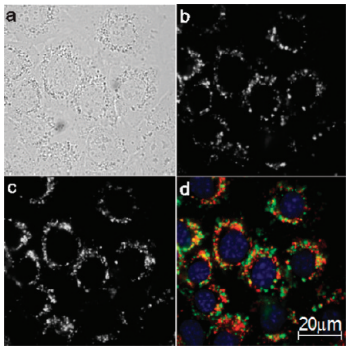

Figure 4. (a) Bright field and fluorescent images of MEFs loaded with 5 μg/mL (b) perylene and 5 μg/mL (c) PtPFPP NPs. Overlaid multicolor images are shown in panel d: PtPFPP, red; perylene, green; Hoechst33342, blue.

loaded with 5−10 μg/mL PtPFPP or perylene NPs for ≥3 h.

Sub-Cellular Localization and Mechanisms of Probe Uptake. First, MEFs were loaded with 5 μg/mL PtPFPP and 5 μg/mL perylene NPs and analyzed by wide-field fluorescence microscopy. Figure 4 shows very similar localization patterns for the two probes: close to the cell nucleus but not penetrating into it. This result and also Figure 3b prove that cellular uptake of the NPs is determined mainly by the polymeric material (RL-100) rather than the dye. Co-staining with transferrin-Alexa488 (clathrin-mediated endosomal stain) of MEF cells loaded with PtPFPP NPs showed only partial colocalization (Supporting Information, Figure S3). The stains for lysosomes, mitochondria, and endoplasmic reticulum showed no colocalization with the NPs. Overall, the NPs resemble the endosomal stain; however, their exact localization cannot be specified conclusively. MEFs loaded with perylene NPs were also analyzed by confocal microscopy, which provides high spatial and 3-D resolution. The probe did not change cell morphology and was detectable already after 3 h of loading (Figure 5a−f). After 18 h, probe localization was similar, but the amounts were higher (Figure 5d,f). Cross sections of the Z-stack confocal images were generated and compared to those of the nuclear stain Hoechst33342 and cell membrane stain bis-(1,3-diethylthiobarbituric acid) trimethine oxonol ($DiSBAC_2(3)$) (costaining with $DiSBAC_2(3)$ was not possible due to spectral overlap). Figure 5g−i further confirm that the NPs are mostly located close to, but not penetrating, the nucleus.

Mechanisms of the NP probe uptake were investigated in individual MEFs by confocal imaging and in cell populations by flow cytometry. TR-F measurements were set aside as they can be influenced by probe nonspecific binding on the surface. Energy dependence of the uptake was investigated by loading the cells: (i) at 4 °C in glucose(+) medium; (ii) at 37 °C in glucose(-)/galactose(+) medium containing oligomycin (Complex V inhibitor). Low temperature is known to decrease endocytosis,[32] while preconditioning with

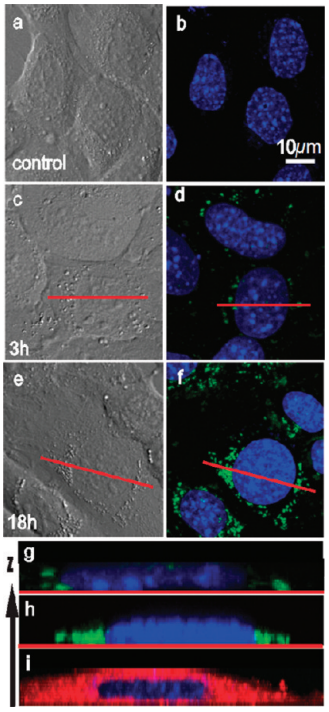

Figure 5. (a,b) DIC and confocal fluorescence images of MEFs stained with Hoechst3342 (blue) and perylene NPs (green) for 3 h (c,d) and 18 h (e,f), and their cross sections (g,h). Red line shows cell diameter. (i) Cross section of MEF cells stained with a plasma membrane stain DiSBAC$_2$(3).

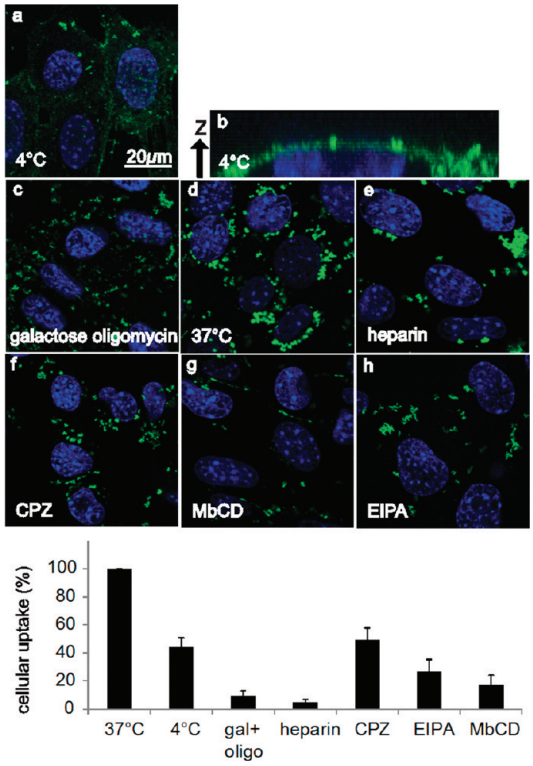

Figure 6. Confocal fluorescent images of MEFs loaded with perylene NPs (green). The effect on probe brightness and localization after 3 h loading at 4 °C: (a) whole image, (b) and cross section; (c) ATP depletion, (d) standard conditions, (e) inhibition of endocytosis with heparin, (f) CPZ, (g) MbCD, and (h) EIPA. (i) FACS analysis of MEFs loaded under different conditions.

galactose/oligomycin significantly reduces cellular ATP levels.[21] For both treatments, imaging revealed the presence of the NPs only on the cell membrane (Figure 6a–c) and significantly reduced loading with respect to control cells (Figure 6d). This shows that NP uptake is energy dependent. The binding of cargo to heparan sulfates (proteoglycans on cell surface) is considered to be the first step in the energy-dependent endocytic pathway,[33] which can be inhibited by heparin. Images of MEFs pretreated with 50 μg/mL heparin showed aggregation of the NPs on cell membrane (Figure 6e), thus suggesting that proteoglycans are involved in the uptake. One should keep in mind that negatively charged heparin can form aggregates with positively charged NPs, so that its inhibitory effect on endocytosis of the NP can be overestimated. To find out what endocytic pathways are involved in the uptake, the cells were pretreated with chlorpromazine (CPZ, 10 μg/mL) and methyl β-cyclodextrin (MbCD, 5 mM)—inhibitors for clathrin and caveolin dependent endocytosis, respectively,[34] or Na^+/H^+ exchanger antagonist 5-(*N*-ethyl-*N*-isopropyl)-amiloride (EIPA, 10 μM)—macropinocytosis inhibitor, and then incubated for 3 h with NPs in the presence of the inhibitor.[35] All these inhibitors were seen to reduce cellular uptake and alter probe localization (Figure 6f–h). A similar reduction in probe loading in MEFs was confirmed by FACS measurements (Figure 6i). These results highlight the complex mechanism of NP uptake, which involves all the main endocytic pathways.

O_2 Calibration of PtPFPP NP Probe. To be able to translate measured lifetime values into icO_2 concentration, the NP probe was calibrated in a biological (*i.e.*, intracellular) environment. MEFs were cultured in a 96-well plate (3×10^4 cells/well), loaded with 10 μg/mL of the NP probe for 14 h and washed. To eliminate local O_2 gradients within the sample, cell respiration was blocked by the addition of 10 μM of AntiA. The plate was then transferred to a hypoxia chamber (Coy Scientific) and measured on the TR-F reader at different levels of atmospheric pO_2 (0–20.88 kPa). After temperature and gas equilibration phosphorescence lifetimes were recorded and used to generate O_2 calibration (Figure 7a). This calibration was fitted with the following function: $[icO_2] = 45.65 \times \ln(41.35/(\tau - 29.62))$, which was used to generate the profiles of icO_2 (see below). In addition, resting respiring MEFs loaded with the NP probe were also measured, and O_2 calibration was used to calculate their *relative* deoxygenation (%) at different pO_2 values (Figure 7b).

Monitoring of Respiratory Responses of Cells to Mitochondrial Uncouplers and Inhibitors. To monitor the dynamics of icO_2 and changes in cellular respiration, MEFs loaded with PtPFPP NPs were treated with classical mitochondrial uncouplers and inhibitors. Figure 8a,b shows profiles of probe lifetime and icO_2 for MEFs cultured

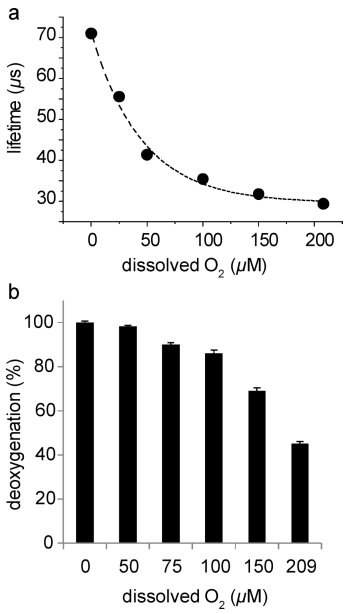

Figure 7. O_2 calibration of the PtPFPP NP probe: (a) phosphorescence lifetime (τ) in nonrespiring MEFs at different external O_2 concentrations (●); (b) relative deoxygenation of respiring MEFs at different dissolved O_2 levels (0−209 μM).

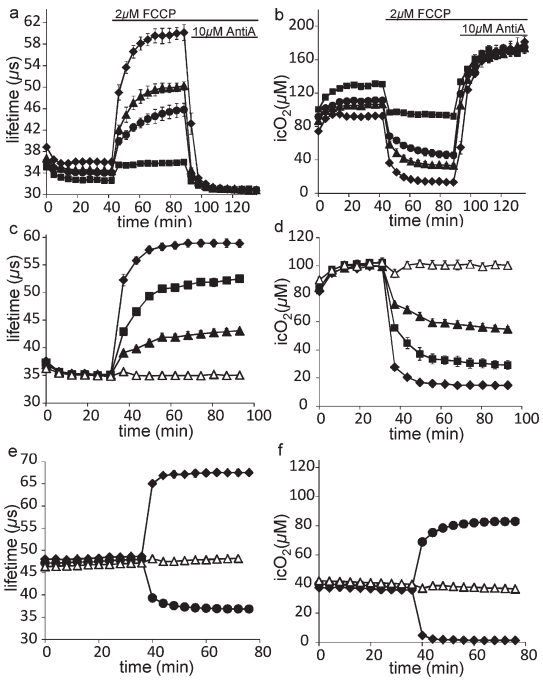

Figure 8. Basal signals for the resting MEFs and their respiratory responses to the addition of 2 μM FCCP followed by 10 μM AntiA at different cell numbers (1×10^4 (■), 2×10^4 (●), 3×10^4 (▲) and 6×10^4 (◆) cells/well), presented in (a) lifetime and (b) O_2 scales. (c,d) The response of 3×10^4 cells/well to 1 (▲), 2 (■), 4 μM (◆) FCCP and carrier (Δ) (in lifetime and icO_2 scales). (e,f) Responses to 2 μM FCCP (◆),10 μM AntiA (●), and carrier (Δ) at 10 kPa pO_2.

at different densities and monitored at pO_2 20.88 kPa, 37 °C with sequential treatment with 2 μM carbonyl cyanide 4-(trifluoromethoxy) phenylhydrazone (FCCP, at 40 min) and 10 μM AntiA (at 90 min). For the resting MEFs seeded at increasing densities (1×10^4 to 8×10^4 cells/well) basal lifetimes were seen to increase from 32.18 ± 0.19 to 35.58 ± 0.30 μs, thus reflecting significantly reduced icO_2 levels within the cell monolayer (between 135 and 90 μM, respectively, while in air-saturated conditions they are expected to be 209 μM).

Upon cell stimulation by the addition of FCCP, the differences in oxygenation of the cell layer become more evident. FCCP uncouples the respiratory chain and oxidative phosphorylation in the mitochondria, which leads to increased rate of O_2 consumption. This causes a deeper deoxygenation of the cells which leveled off at ~10 μM O_2 at high cell numbers. The associated changes in icO_2 correspond to the transition of the respiring sample to a new steady state, where O_2 consumption by the cells is again balanced by O_2 diffusion from the medium and gaseous atmosphere.[13] The process of re-establishment of new O_2 gradients in the respiring samples upon cell stimulation can also be monitored as an increase in phosphorescence lifetime of the NP probe loaded in MEFs.

Strong dependence of measured icO_2 concentrations and responses to metabolic stimulation on the density of cell monolayer also points to the fact that in such samples with respiring MEFs (monitored at 21 kPa of atmospheric pO_2) global O_2 gradients dominate over the microscopic O_2 gradients within the cells. Otherwise, the icO_2 levels would be seen independent of the cell density.

The subsequent addition of AntiA (inhibitor of Complex III of the electron transport chain which blocks cellular respiration) led to gradual dissipation of O_2 gradients within the sample, so that icO_2 approached air-saturated levels. This can be seen as a decrease in probe lifetime to about ~30.38 ± 0.09 μs, that is, below the levels of resting respiring MEFs. In the presence of AntiA, lifetime values (and icO_2) in all the different samples became equal and independent of the cell number. FCCP and AntiA had no effect on the NP probe itself (data not shown).

Figure 8c,d shows dose response of MEF cells to FCCP in the lifetime and icO_2 scales. The addition of 1−4 μM FCCP was seen to activate and constantly increase cell respiration in a concentration dependent manner. The addition of AntiA decreased the lifetime and iO_2 values to the level of air-saturation. As expected, control MEF cells treated with carrier only (DMSO) showed practically no changes in the lifetime, but only minor temperature equilibration effects associated with plate withdrawal from the instrument and addition of drugs.

Lastly, the probe was applied to monitor icO_2 levels in MEFs in hypoxic macro-environment. Oxygenation of resting MEFs and the effects of FCCP, AntiA, and carrier treatments were monitored in the hypoxia chamber preset at 15 and 10 kPa pO_2 (approximately

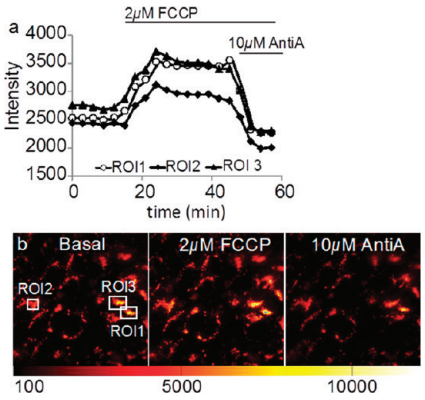

Figure 9. Time-lapse fluorescent imaging of MEFs and their responses to metabolic stimulation using the PtPFPP NP probe: (a) intensity profiles for the three regions of interest (ROI), and (b) corresponding images for the basal condition, uncoupled with 2 μM FCCP and inhibited with 10 μM AntiA (correspond to plateau regions on panel a).

150 μM and 100 μM dissolved O_2 in saturated medium, respectively). As expected, under these conditions resting icO_2 levels were significantly reduced compared to normoxic macro-environment, 21 kPa (Figure 8e,f), and the responses to cell stimulation became amplified. The difference in oxygenation between resting and nonrespiring (AntiA treated) cells also increased (see Figure 7b). The addition of 2 μM FCCP at 10 kPa pO_2 resulted in almost complete deoxygenation of the cell layer.

One can therefore see that the PtPFPP NP probe produces the anticipated results on icO_2 levels in MEFs as well as the other cells (data not shown), and robust responses to cell stimulation with classical mitochondrial effectors/drugs. It allows reliable and reproducible monitoring of cell oxygenation and its changes associated with altered cell metabolism, with high accuracy and using commercial multilabel readers with TR-F capabilities, without any modifications. The results produced are in good agreement with the mode of action of the effectors used and with the data generated using the other O_2 probes.[13]

icO_2 Imaging Experiments. High brightness, photostability, and high self-loading ability of the PtPFPP NP probe with various mammalian cells allow its use in O_2 imaging experiments on fluorescent microscopes. For accurate assessment of icO_2 concentration, phosphorescence lifetime modality (*i.e.*, microsecond FLIM) is preferred;[6,36,37] however, such systems are not widely available. At the same time, we demonstrate that even in intensity mode the PtPFPP NP probe shows quite satisfactory performance in O_2 imaging experiments, providing good spatial resolution, relatively short exposure time (50 ms/frame) and prolonged monitoring (60 min and more) and single cell analysis capabilities. Figure 9 shows monitoring of *relative* oxygenation and respiratory responses of MEFs to stimulation in fluorescence intensity mode (at 20 kPa pO_2). After recording of basal signal from three individual cells for 10–20 min, the sample was treated with FCCP, and when the response reached its plateau AntiA treatment was applied. The experiment was carried out as described previously.[37] Similar to the experiments on the TR-F reader (see Figure 8c,d), the phosphorescence intensity readings of the NP probe correlated with icO_2 levels (inverse relationship). One can see that the profiles of the NP probe signal generated on the microscope are similar to those produced on the TR-F reader. At the same time, conversion into icO_2 concentrations is somewhat more difficult here, since the intensity calibration of the probe is not as stable and accurate as the lifetime calibration on the TR-F reader. Figure 9b shows the intensity changes in the images according to the treatment with FCCP and AntiA.

CONCLUSIONS

The NP probe based on PtPFPP O_2-sensitive dye and Eudragit RL-100 polymer, which is very easy to produce and use, demonstrates excellent self-loading ability with many common lines of mammalian cells. Simple incubation of the probe with test cells in common growth media over a short period of time (3–12 h) produces high and stable phosphorescent intensity signals. Cellular uptake of the NPs occurs by endocytosis in an energy dependent manner, and this process is rather independent of the type of luminescent dye incorporated in the NPs. In loaded cells the NPs localize close to cell nucleus and partly colocalize with endosomes. The localization pattern is not influenced much by the loading time. Within the optimized range of working concentrations and loading times, toxic effects of the probe on cells are negligible.

The NP probe loaded in the cells allows reliable and accurate measurement of icO_2 concentration in adherent cell cultures, by relatively simple means. Phosphorescence lifetime measurements on a commercial TR-F reader provide reliable and accurate monitoring of cell oxygenation and metabolic responses of respiring cells. Measured lifetime profiles can be converted into icO_2 concentrations using O_2 calibration generated in a separate (once off) experiment. Photostability and brightness of the NP probe is superior to the other O_2 probes currently in use, therefore it is better suited for microscopy imaging experiments, where O_2 can be imaged in individual cells and tissue slices. The PtPFPP NP probe complements the extracellular O_2 probes currently used to measure oxygen consumption rates (end-point assay). It can be used in a high throughput screening format (TR-F reader) and on high content live cell imaging systems, to generate useful real-time information on cellular responses to drugs and metabolic stimulation.

Overall, it provides a powerful tool for studies of mitochondrial and cellular function, cell metabolism, bioenergetics, hypoxia research and various disease models.

MATERIALS AND METHODS

Materials. Eudragit RL-100 copolymer (poly-(ethylacrylate, methyl-methacrylate, and chloro-trimethyl-aminoethyl methacrylate), M.W. ≈ 150 000D, 8.8−12% of quaternary ammonium groups) was from Degussa, Germany. PtPFPP dye was from Frontier Scientific. OptiMEM I medium, $DiSBAC_2(3)$, Hoechst 33342, MitoTrackerGreen (MTG), LysoTrackerGreen (LTG), ERTrackerGreen (ETG), and transferrin-Alexa Fluor488 stains were from Invitrogen (Carlsbad, CA). DMEM, Roswell Park Memorial Institute Medium (RPMI), collagen IV, poly-D-lysine, oligomycin, MbCD, EIPA, CPZ, FCCP, AntiA, and all the other reagents were from Sigma-Aldrich. Plasticware was from Sarstedt (Ireland), MatTek (Ashland, MA), Greiner Bio One (Germany), Becton Dickinson (Biosciences, Ireland), and IBIDI (Munich, Germany). The pH-Xtra probe for the measurement of extracellular acidification was from Luxcel Biosciences (Ireland). Cellular ATP assay, CellTiter-Glo, and cell membrane integrity assay, CytoTox-ONE, were from Promega (Madison, WI). BCA Protein Assay kit was from Thermo Fisher Scientific (Rockford, IL). 1,6,7,12-Tetrachloro-*N*,*N*′-di-(2,6-diisopropylphenyl)-perylene-3,4:9,10-tertracarboxylic bisimide (perylene) was prepared according to the procedure in ref 38.

Preparation of Phosphorescent and Fluorescent Nanoparticles. A 1.5 g portion of RL-100 polymer and 22.5 mg of PtPFPP was dissolved in 750 g of acetone. This solution was placed in a 5 L beaker to which 4 L of deionized water were added over 20 s under rigorous stirring. Acetone was subsequently removed under reduced pressure and an aqueous dispersion of the NP was further concentrated to approximately 75 mL. Traces of aggregates were removed by filtration through a paper filter and then through a sterile 0.22 μm filter. Thus, stock of the O_2 probe was produced, which had NP concentration of 10 mg/mL (1.5% w/w PtPFPP), size of approximately 30 nm, Z-potential of +58 mV, as determined on a particle size analyzer Zetasizer Nano ZS (Malvern Instruments, Germany). It showed a bright phosphorescence in aqueous solution which was quenched by O_2. This solution was stored in a dark place at +4 °C for further use. The fluorescent NP probe doped with perylene dye was prepared using the same method, but with 15 mg of perylene instead of PtPFPP.

SEM *and AFM* were used to characterize the morphology and size of the polymeric NPs. SEM imaging was done on a Zeiss Ultra 55 system, using aqueous dispersion of the NPs pipetted on a sliced mica support, subsequently rinsed with water and conducted with Au and Pt. AFM images were generated on a Veeco Dimension 3100 combined with NanoScope IVa (NSIVa) Scanning Probe Microscope controller and a hybrid XYZ scanner, using a diluted sample of the NPs (0.0001% w/w) fast dried onto freshly cleaved mica and analyzed in tapping mode with Olympus OMCL-AC240/AC160 tips.

Optical Measurements. Absorption spectra of the NP probes were measured on an HP8453 diode array spectrophotometer (Agilent) in 1 cm quartz cell. Excitation and emission spectra were measured on an LS-50B fluorescence spectrometer (Perkin-Elmer). TR-F intensity and phosphorescence lifetime measurements, O_2 calibration and intracellular O_2 sensing experiments with PtPFPP NP probe were conducted on Victor multilabel reader with TR-F capabilities (Perkin-Elmer), as described previously.[16]

Cell Culture and Loading with the NP Probes. MEFs, HepG2, HeLa, PC12 and SH-SY5Y cell lines obtained from the American Collection of Cell Cultures were grown in 75 cm^2 flasks. MEF, HepG2, HeLa and SH-SY5Y cells were cultured in DMEM supplemented with 10% FBS, 2 mM L-glutamine, 100 U/mL penicillin and 100 mg/mL streptomycin (P/S), at 37 °C under humid conditions with 5% CO_2. PC12 cells were cultured in RPMI-1640 medium supplemented with 2 mM L-glutamine, 10% horse serum (HS), 5% FBS, and P/S, under the same conditions. For the O_2, ATP, LDH, and ECA measurements, cells were seeded on 96 well plates (Sarstedt) coated with collagen IV at 2−6 × 10^4 cells/well. For live cell imaging experiments, cells were seeded at 1−3 × 10^4 cells/well on glass-bottom mini-dishes (MatTek) or mini-chambers with a 2-well insert (IBIDI), both coated with a mixture of collagen IV (0.007%) and poly-D-lysine (0.003%).

Loading was achieved by simple incubation of the cells with 1−40 μg/mL of PtPFPP or perylene NP probe in corresponding growth media (the same volume as in culturing), for 3−24 h in CO_2 incubator at 37 °C. After incubation, loaded cells were washed once and then measured in fresh medium (without phenol red) supplemented with 20 mM HEPES, pH 7.4 (to maintain physiological pH in CO_2-free environment).

Probe Localization and Mechanisms of Uptake Studies. MEF, PC12, HepG2, SH-SY5Y, and HeLa cells seeded on MatTek dishes at subconfluent densities were loaded by incubating them with the NP probe (1−40 μg/mL for 3−24 h for kinetic studies or for 3 h for inhibition studies). Then the cells were washed with prewarmed measurement medium (see above) and analyzed. To allow plasma membrane and mitochondrial membrane visualization, cells were additionally stained in OptiMEM I medium with 1 μM $DiSBAC_2(3)$ and 20 nM TMRM, respectively. For the samples loaded with NPs and $DiSBAC_2(3)$, cell nuclei were stained with 1 μM Hoechst 33342. During the measurements, $DiSBAC_2(3)$ probes were maintained in solution at 0.25 μM, respectively. To study intracellular localization of the NP probe, loaded MEFs were costained with either 25 nM MTG, 100 nM LTG, 1 μM ETG, or 40 μg/mL transferrin-AlexaFluo488, together with 1 μM Hoechst 33342. All staining was performed according to manufactures instructions. To determine the effects of temperature on the NP uptake, MEF cells were preincubated 30 min at 4 °C and loaded with NP for 3 h at 4 °C. The effect ATP depletion on the uptake was studied by incubating the cells in galactose media for 2 h, treating them with 10 μM oligomycin for 30 min, loading with the NP probe in the presence of oligomycin and then measuring. Involvement of cellular proteoglycans in NP uptake was studied by incubating the cells with 50 μg/mL heparin for 30 min, followed by incubation with 10 μg/mL NP for 3 h in the presence of heparin. To study the effects of endocytosis inhibitors, MEF cells were preincubated for 30 min with 50 μM 5 EIPA, 5 mM MbCD, or 10 μg/mL CPZ drug, followed by 3 h incubation with the NP in the presence of the inhibitor and measurement.

Microscopy Imaging. Live cell fluorescence microscopy imaging was conducted on an Olympus FV1000 confocal laser scanning microscope with controlled CO_2, humidity, and temperature. Acquisition of each spectral signal was done in sequential laser mode with emission gates adjusted to avoid overlaps. The perylene dye was excited at 488 nm (1.5−5% of laser power) with emission collected at 500−550 nm. Hoechst 33342 was excited at 405 nm (3% laser power) with emission collected at 440−480 nm. $DiSBAC_2(3)$ was excited at 543 nm (5%, 1.5% power, respectively) collecting the emission with a 555−600 nm filter. In all the experiments fluorescent and differential interference contrast (DIC) images were collected with a 60× oil immersion objective using 0.5 μm steps. The resulting *z*-stacked images were analyzed using FV1000 Viewer (Olympus).

Images of the cells loaded with PtPFPP and perylene-doped NPs were generated on a wide-field fluorescence microscope Axiovert 200 (Carl Zeiss, Germany) equipped with an LED excitation module (390 nm LED for PtPFPP and 470 nm LED for perylene) and intensified CCD camera (LaVision BioTec, Germany). The LEDs were pulsed with a fixed pulse length of 10 μs. Images of cells loaded with PtPFPP and perylene NPs were generated using 655/50 and 535/50 nm emission bandpass filters, respectively. Fluorescence intensity was integrated over a light exposure

time of 50 ms. In PtPFPP NP colocalization experiments, MTG, LTG, ETG, and transferrin-AlexaFluo488 images were generated under constant illumination (488 nm LED) with a fluorescence integration time of 100 ms/frame in combination with 535/50 nm emission bandpass filter. Images of the nuclear stain Hoechst 33342 were acquired under pulsed 390 nm LED excitation with an integration time of 50 ms/frame and DAPI filter set (387 ± 11/447 ± 60 nm). Images were taken on EC PanNeofluar 40x/1.30 oil immersion objective, processed with ImSpector software (LaVision), and then with Adobe Photoshop and Illustrator software.

Flow Cytometry. MEFs were seeded on 35 mm Petri dishes coated with collagen IV, then treated and loaded in the same manner as for confocal microscopy, washed two times in PBS, trypsinsed, resuspended in 1 mL PBS, passed through a 21G needle to break aggregates and transferred into 5 mL polystyrene tubes. Samples were analyzed on a fluorescence activated cell sorter FACSCalibur (Becton Dickinson, NJ) using 488 nm laser for excitation, and CellGate software for data analysis.

Intracellular O_2 Sensing Experiments. MEFs were seeded in 96-well plates, loaded with 5−10 μg/mL of PtPFPP NPs for 3−24 h in regular medium and then washed. Intracellular O_2 sensing experiments were conducted on a Victor reader at 37 °C using 340 nm excitation and 642 nm emission filters. Typically, 24−48 wells with cells in 90 μL of air-saturated medium supplemented with 20 mM HEPES, pH 7.4, were monitored simultaneously. Each sample well was measured repetitively every 1−6 min by taking two TR-F intensity readings at delay times of 30 and 70 μs and gate time 100 μs. Measured TR-F intensity signals for each sample well were converted into phosphorescence lifetime (τ) values: $\tau = (t_1 - t_2)/\ln(F_1/F_2)$, where τ is probe fluorescence lifetime, t_1, t_2 are the two delay times, and F_1, F_2 are the corresponding TR-F intensity signals, and plotted as time profiles.[16]

When recording respiratory responses to stimulation, the plate with loaded cells was initially monitored for 10−40 min to reach gas and temperature equilibrium and obtain basal icO_2 signals. Then the plate was quickly withdrawn from the reader, compounds were added to the cells (10 μL of 10× stock solution per well) and monitoring was resumed. The resulting TR-F signals were converted into lifetime profiles for each sample well. These profiles were subsequently converted into icO_2 concentration (μM), using the calibration function of the icO_2 NP probe. Necessary controls (without cells, without probe) and samples with respiring cells were incorporated as appropriate.

Calibration of the PtPFPP NP probe was performed directly in live cells on the TR-F reader placed in a hypoxia chamber (Coy Scientific) which was sequentially equilibrated at different pO_2: 1.0−20.88 kPa. The cells were treated with 10 μM AntiA to inhibit respiration and ensure that their icO_2 levels are equal to the external O_2 determined by the settings of the hypoxia chamber. Following ~30 min of temperature and gas equilibration of the plate at the selected pO_2, steady-state TR-F intensity readings were recorded for the samples containing nonrespiring cells preloaded with the NP probe. Since hypoxia chambers are difficult to equilibrate below 2% O_2, a zero O_2 calibration point was produced by chemical deoxygenation with glucose oxidase enzyme (0.1 mg/mL). Corresponding lifetime values were calculated and plotted against O_2 concentration in the medium at given pO_2 (20.88 kPa pO_2 in air corresponds to 209 μM O_2 in solution at +37 °C). The resulting set of data points was fitted with a mathematical function (giving the best R^2), which was subsequently used as calibration function to convert measured lifetime values into icO_2 concentration.

icO_2 imaging experiments with MEF cells were performed on the wide field fluorescence microscope Zeiss Axiovert 200, in intensity mode. There were 3×10^4 cells in 70 μL of medium seeded into glass bottom imaging dishes (Matek) with double-chamber culturing inserts (Ibidi, Germany), grown for at least 24 h to a confluent monolayer, incubated with 10 μg/mL PtPFPP NP for more than 3 h, washed once, and then measured in 70 μL of DMEM at 37 °C. After a stable basal signal in the selected region of interest (ROI) with resting cells was obtained, the incubation chamber lid was gently opened, 7 μL of 10× drug stock (FCCP and Anti A) were added to cells, and monitoring was resumed. Images for individually chosen ROIs taken periodically over 60 min were extracted, exported, and processed to generate phosphorescence intensity images and time profiles.

ECA Assay. The ECA rate was monitored as described.[12] Briefly, MEFs were seeded and loaded with the PtPFPP NP probe in standard conditions. Then medium was replaced with unbuffered DMEM, supplemented with 1 mM sodium pyruvate and 10 mM glucose, pH 7.4 (ECA measurement buffer), and cells were maintained in a CO_2-free incubator at 37 °C for 3 h to release absorbed CO_2. Then the medium was replaced with 100 μL of fresh ECA medium containing 2 μM of pH-Xtra probe, and the plate was measured kinetically on the Victor reader at 37 °C for 30−90 min using the TR-F mode and Europium filter set (340 ± 35 nm excitation and 615 ± 8.5 nm emission). Each time TR-F intensity signals were measured at two delay times of 100 and 300 μs and a measurement window of 30 μs and converted into lifetime values: $\tau = (t_1 - t_2)/\ln(F_1/F_2)$. To determine relative changes in the ECA, lifetime changes of the pH-Xtra probe (*i.e.*, $d\tau/dt$) for treated samples were compared to that of untreated controls.

ATP, LDH, and Protein Content. Cellular ATP was measured using CellTiter-Glo Assay kit in white 96-well plate (Greiner Bio One), using Victor reader and standard chemiluminescence settings. Cell membrane integrity after loading with NP was tested using CytoTox-ONE Assay kit (LDH release) and clear bottom 96-well plates (Greiner Bio One). Signals for unloaded cells were taken as 100% viability. Total protein content was determined using BCA Protein Assay kit. These assays were conducted according to manufacturers' protocols.

Statistics. All the results are presented as mean values ± standard deviation (error bars on the plots), usually for 6−8 replicates (sample wells). Imaging data are presented as average values for 3−10 individual cells. Each experiment was repeated 3−5 times to ensure consistency of results.

Acknowledgment. Financial support of this work by the Science Foundation of Ireland, Grant 07/IN.1/B1804, and by the European Commission (FP7 projects NMP4-SL-2008-214706 and MC-IAPP-2009-230641) is gratefully acknowledged. Authors thank Dr. H. Plank (Institute for Electron Microscopy and Fine Structure Research, TU Graz) and K. Koren (Institute of Analytical and Food Chemistry, TU Graz) for the help with SEM and AFM.

Supporting Information Available: Effect of pH and ionic strength on the lifetime of PtPFPP-doped NPs; leaking of the NP probe from the cells; changes in viability (total ATP) and extracellular acidification for MEF cells loaded with the NPs (Figure S1). NP uptake in different cell lines (Figure S2). Wide field fluorescence images of MEF cells loaded with PtFPP NP and costained with the endosomal and nuclear stains (Figure S3). This material is available free of charge *via* the Internet at http://pubs.acs.org.

REFERENCES AND NOTES

1. Lee, Y. E.; Smith, R.; Kopelman, R. Nanoparticle PEBBLE Sensors in Live Cells and In Vivo. *Annu. Rev. Anal. Chem.* **2009**, *2*, 57–76.
2. Semenza, G. L. Life with Oxygen. *Science* **2007**, *318*, 62–64.
3. Aragones, J.; Fraisl, P.; Baes, M.; Carmeliet, P. Oxygen Sensors at the Crossroad of Metabolism. *Cell Metab.* **2009**, *9*, 11–22.
4. Wu, C. C.; Luk, H. N.; Lin, Y. T.; Yuan, C. Y. A Clark-Type Oxygen Chip for *in Situ* Estimation of the Respiratory Activity of Adhering Cells. *Talanta* **2010**, *81*, 228–234.
5. Liu, Y.; Villamena, F. A.; Sun, J.; Wang, T. Y.; Zweier, J. L. Esterified Trityl Radicals as Intracellular Oxygen Probes. *Free Radical Biol. Med.* **2009**, *46*, 876–883.
6. Rumsey, W. L.; Vanderkooi, J. M.; Wilson, D. F. Imaging of Phosphorescence: A Novel Method for Measuring Oxygen Distribution in Perfused Tissue. *Science* **1988**, *241*, 1649–1651.
7. Papkovsky, D. B. Methods in Optical Oxygen Sensing: Protocols and Critical Analyses. *Methods Enzymol.* **2004**, *381*, 715–735.
8. Wilson, D. F. Quantifying the Role of Oxygen Pressure in Tissue Function. *Am. J. Physiol.* **2008**, *294*, H11–H13.

9. Ji, J.; Rosenzweig, N.; Jones, I.; Rosenzweig, Z. Molecular Oxygen-Sensitive Fluorescent Lipobeads for Intracellular Oxygen Measurements in Murine Macrophages. *Anal. Chem.* **2001**, *73*, 3521–3527.
10. Ferrick, D. A.; Neilson, A.; Beeson, C. Advances in Measuring Cellular Bioenergetics Using Extracellular Flux. *Drug. Discov. Today* **2008**, *13*, 268–274.
11. Ceroni, P.; Lebedev, A. Y.; Marchi, E.; Yuan, M.; Esipova, T. V.; Bergamini, G.; Wilson, D. F.; Busch, T. M.; Vinogradov, S. A. Evaluation of Phototoxicity of Dendritic Porphyrin-Based Phosphorescent Oxygen Probes: An *in Vitro* Study. *Photochem. Photobiol. Sci.* **2011**, *10*, 1056–1065.
12. Hynes, J.; Natoli, E., Jr.; Will, Y. Fluorescent pH and Oxygen Probes of the Assessment of Mitochondrial Toxicity in Isolated Mitochondria and Whole Cells. *Curr. Protoc. Toxicol.* **2009**, *40*, 2.16.1–2.16.22.
13. Zhdanov, A. V.; Dmitriev, R. I.; Papkovsky, D. B. Bafilomycin A1 Activates Respiration of Neuronal Cells *via* Uncoupling Associated with Flickering Depolarization of Mitochondria *Cell. Mol. Life Sci.* **2010**, *68*, 903–917.
14. Kindig, C. A.; Howlett, R. A.; Hogan, M. C. Effect of Extracellular PO_2 on the Fall in Intracellular PO_2 in Contracting Single Myocytes. *J. Appl. Physiol.* **2003**, *94*, 1964–1970.
15. O'Riordan, T. C.; Fitzgerald, K.; Ponomarev, G. V.; Mackrill, J.; Hynes, J.; Taylor, C.; Papkovsky, D. B. Sensing Intracellular Oxygen Using Near-Infrared Phosphorescent Probes and Live-Cell Fluorescence Imaging. *Am. J. Physiol.* **2007**, *292*, R1613–R1620.
16. O'Riordan, T. C.; Zhdanov, A. V.; Ponomarev, G. V.; Papkovsky, D. B. Analysis of Intracellular Oxygen and Metabolic Responses of Mammalian Cells by Time-Resolved Fluorometry. *Anal. Chem.* **2007**, *79*, 9414–9419.
17. Schmalzlin, E.; van Dongen, J. T.; Klimant, I.; Marmodee, B.; Steup, M.; Fisahn, J.; Geigenberger, P.; Lohmannsroben, H. G. An Optical Multifrequency Phase-Modulation Method Using Microbeads for Measuring Intracellular Oxygen Concentrations in Plants. *Biophys. J.* **2005**, *89*, 1339–1345.
18. Koo, Y. E.; Cao, Y.; Kopelman, R.; Koo, S. M.; Brasuel, M.; Philbert, M. A. Real-Time Measurements of Dissolved Oxygen Inside Live Cells by Organically Modified Silicate Fluorescent Nanosensors. *Anal. Chem.* **2004**, *76*, 2498–2505.
19. Wu, C.; Bull, B.; Christensen, K.; McNeill, J. Ratiometric Single-Nanoparticle Oxygen Sensors for Biological Imaging. *Angew. Chem.* **2009**, *121*, 2779–2783.
20. Kindig, C. A.; Walsh, B.; Howlett, R. A.; Stary, C. M.; Hogan, M. C. Relationship between Intracellular PO_2 Recovery Kinetics and Fatigability in Isolated Single Frog Myocytes. *J. Appl. Physiol.* **2005**, *98*, 2316–2319.
21. Dmitriev, R. I.; Ropiak, H. M.; Yashunsky, D. V.; Ponomarev, G. V.; Zhdanov, A. V.; Papkovsky, D. B. Bactenecin 7 Peptide Fragment as a Tool for Intracellular Delivery of a Phosphorescent Oxygen Sensor. *FEBS J.* **2010**, *277*, 4651–4661.
22. Dmitriev, R. I.; Zhdanov, A. V.; Ponomarev, G. V.; Yashunski, D. V.; Papkovsky, D. B. Intracellular Oxygen-Sensitive Phosphorescent Probes Based on Cell-Penetrating Peptides. *Anal. Biochem.* **2010**, *398*, 24–33.
23. Koo Lee, Y.-E.; Ulbrich, E. E.; Kim, G.; Hah, H.; Strollo, C.; Fan, W.; Gurjar, R.; Koo, S.; Kopelman, R. Near Infrared Luminescent Oxygen Nanosensors with Nanoparticle Matrix Tailored Sensitivity. *Anal. Chem.* **2010**, *82*, 8446–8455.
24. Wang, X.-d.; Gorris, H. H.; Stolwijk, J. A.; Meier, R. J.; Groegel, D. B. M.; Wegener, J.; Wolfbeis, O. S. Self-Referenced RGB Colour Imaging of Intracellular Oxygen. *Chem. Sci.* **2011**, *2*, 901–906.
25. Bodmeier, R.; Chen, H.; Tyle, P.; Jarosz, P. Spontaneous Formation of Drug-Containing Acrylic Nanoparticles. *J. Microencapsulation* **1991**, *8*, 161–170.
26. Khalil, G.; Gouterman, M.; Ching, S.; Costin, C.; Coyle, L.; Gouin, S.; Green, E.; Sadilek, M.; Wan, R.; Yearyean, J.; Zelelow, B. Synthesis and Spectroscopic Characterization of Ni, Zn, Pd, Pt Tetra(pentafluorophenyl) Porpholactone with Comparisons to Mg, Zn, Y, Pd, Pt Metal Complexes of Tetra(pentafluorophenyl) Porphine. *J. Porphyrins Phtalocyanines* **2002**, *6*, 135–145.
27. Amao, Y.; Miyashita, T.; Okura, I. Platinum Tetrakis(pentafluorophenyl)porphyrin Immobilized in Polytrifluoroethylmethacrylate Film as a Photostable Optical Oxygen Detection Material. *J. Fluorine Chem.* **2001**, *107*, 101–106.
28. Das, S.; Suresh, P. K.; Desmukh, R. Design of Eudragit RL-100 Nanoparticles by Nanoprecipitation Method for Ocular Drug Delivery. *Nanomed. Nanotechnol.* **2010**, *6*, 318–323.
29. Borisov, S. M.; Mayr, T.; Mistlberger, G.; Waich, K.; Koren, K.; Chojnacki, P.; Klimant, I. Precipitation as a Simple and Versatile Method for Preparation of Optical Nanochemosensors. *Talanta* **2009**, *79*, 1322–1330.
30. van der Aa, M.; Huth, U.; Häfele, S.; Schubert, R.; Oosting, R.; Mastrobattista, E.; Hennink, W.; Peschka-Süss, R.; Koning, G.; Crommelin, D. Cellular Uptake of Cationic Polymer–DNA Complexes *via* Caveolae Plays a Pivotal Role in Gene Transfection in COS-7 Cells. *Pharm. Res.* **2007**, *24*, 1590–1598.
31. Lesniak, A.; Campbell, A.; Monopoli, M. P.; Lynch, I.; Salvati, A.; Dawson, K. A. Serum Heat Inactivation Affects Protein Corona Composition and Nanoparticle Uptake. *Biomaterials* **2010**, *31*, 9511–9518.
32. Zobel, H. P.; Stieneker, F.; Atmaca-Abdel Aziz, S.; Gilbert, M.; Werner, D.; R. Noe, C.; Kreuter, J.; Zimmer, A. Evaluation of Aminoalkylmethacrylate Nanoparticles as Colloidal Drug Carrier Systems. Part II: Characterization of Antisense Oligonucleotides Loaded Copolymer Nanoparticles. *Eur. J. Pharm. Biopharm.* **1999**, *48*, 1–12.
33. Poon, G. M.; Gariepy, J. Cell-Surface Proteoglycans as Molecular Portals for Cationic Peptide and Polymer Entry into Cells. *Biochem. Soc. Trans.* **2007**, *35*, 788–793.
34. Harush-Frenkel, O.; Debotton, N.; Benita, S.; Altschuler, Y. Targeting of Nanoparticles to the Clathrin-Mediated Endocytic Pathway. *Biochem. Biophys. Res. Commun.* **2007**, *353*, 26–32.
35. Luehmann, T.; Rimann, M.; Bittermann, A. G.; Hall, H. Cellular Uptake and Intracellular Pathways of PLL-g-PEG-DNA Nanoparticles. *Bioconjugate Chem.* **2008**, *19*, 1907–1916.
36. Sakadzic, S.; Roussakis, E.; Yaseen, M. A.; Mandeville, E. T.; Srinivasan, V. J.; Arai, K.; Ruvinskaya, S.; Devor, A.; Lo, E. H.; Vinogradov, S. A.; Boas, D. A. Two-Photon High-Resolution Measurement of Partial Pressure of Oxygen in Cerebral Vasculature and Tissue. *Nat. Methods* **2010**, *7*, 755–759.
37. Fercher, A.; O'Riordan, T. C.; Zhdanov, A. V.; Dmitriev, R. I.; Papkovsky, D. B. Imaging of Cellular Oxygen and Analysis of Metabolic Responses of Mammalian Cells. *Methods Mol. Biol.* **2010**, *591*, 257–273.
38. Klok, H.-A.; Hernández, J. R.; Becker, S.; Müllen, K. Star-Shaped Fluorescent Polypeptides. *J. Polym. Sci. A1* **2001**, *39*, 1572–1583.